THE ASTROPHYSICAL JOURNAL, 436:229–238, 1994 November 20

EGRET HIGH-ENERGY GAMMA-RAY PULSAR STUDIES. I. YOUNG SPIN-POWERED PULSARS

D. J. THOMPSON,[1] Z. ARZOUMANIAN,[2] D. L. BERTSCH,[1] K. T. S. BRAZIER,[3,4] J. CHIANG,[5,6] N. D'AMICO,[7] B. L. DINGUS,[1,8] J. A. ESPOSITO,[1,8] J. M. FIERRO,[5] C. E. FICHTEL,[1] R. C. HARTMAN,[1] S. D. HUNTER,[1] S. JOHNSTON,[9,10] G. KANBACH,[3] V. M. KASPI,[2] D. A. KNIFFEN,[11] Y. C. LIN,[5] A. G. LYNE,[12] R. N. MANCHESTER,[9] J. R. MATTOX,[1,13] H. A. MAYER-HASSELWANDER,[3] P. F. MICHELSON,[5] C. VON MONTIGNY,[3] H. I. NEL,[14] D. J. NICE,[2] P. L. NOLAN,[5] P. V. RAMANAMURTHY,[1,15] S. L. SHEMAR,[12] E. J. SCHNEID,[16] P. SREEKUMAR,[1,8] AND J. H. TAYLOR[2]

Received 1994 January 14; accepted 1994 May 26

ABSTRACT

As part of its ongoing survey of the high-energy gamma-ray sky, the Energetic Gamma Ray Experiment Telescope (EGRET) on the *Compton Gamma Ray Observatory* has searched for emission from spin-powered pulsars, five of which have now been detected in the energy range 30 MeV $\leq E \leq$ 20 GeV. A systematic study of the all-sky survey has found no additional pulsed gamma-ray sources. The pulsar detections, coupled with the upper limits on pulsed gamma radiation from other radio pulsars, indicate that the simplest models of gamma-ray pulsars are incomplete.

Subject headings: gamma rays — pulsars: general

1. INTRODUCTION

Following the *SAS 2* and *COS B* high-energy gamma-ray observations of the Crab (PSR B0531+21) and Vela (PSR B0833−45) pulsars (e.g., Thompson et al. 1977; Kanbach et al. 1980), searches were conducted in these data sets for additional gamma-ray pulsars (Ögelman et al. 1976; Thompson et al. 1983; Buccheri et al. 1983). Although no additional positive results were found, a variety of calculations indicated that gamma-ray emission is likely from other rotation-powered pulsars (e.g., Harding 1981; Ruderman & Cheng 1988), and these pulsars may make a significant contribution to the Galactic gamma radiation (Bailes & Kniffen 1992).

Instruments on the *Compton Gamma Ray Observatory* have raised the number of known gamma-ray pulsars to six. PSR B1509−58 has been seen between 60 keV and 2 MeV by BATSE, the Burst and Transient Source Experiment (Wilson et al. 1993), OSSE, the Oriented Scintillation Spectrometer Experiment (Ulmer et al. 1993), and COMPTEL, the Imaging Compton Telescope (Bennett et al. 1993), but not by EGRET, the *Energetic Gamma-Ray Experiment Telescope*, at energies above 30 MeV (Brazier et al. 1994). PSR B1706−44 has been detected above 100 MeV by EGRET (Thompson et al. 1992), and PSR B1055−52 is also seen by EGRET, primarily above 300 MeV (Fierro et al. 1993). Neither of these has been reported by the other instruments on the *Compton Observatory*. Geminga (PSR J0633+1746) was found to pulse at energies above 30 MeV by EGRET (Bertsch et al. 1992) following the detection of pulsations in the *ROSAT* X-ray data by Halpern & Holt (1992). Subsequent studies found the Geminga pulsations in the original *SAS 2* (Mattox et al. 1992) and *COS B* data (Bignami & Caraveo 1992; Hermsen et al. 1992). The COMPTEL group (Bennett et al. 1993), in a search of pulsars with high $\dot{E}/D^2$, where $\dot{E}$ is the spin-down energy and D is the distance to the pulsar, has reported indications of pulsations ($3\ \sigma$) from PSR B1951+32 and PSR B0740−28 in the energy range below 30 MeV. At present, these possible detections remain unconfirmed. Ulmer & Schroeder (1994) used OSSE data to compute upper limits to low-energy gamma-ray emission for 15 pulsars and compare those limits with the results for detected pulsars. They conclude that no simple correlation can be found between gamma-ray luminosity and other measured pulsar properties.

This work describes the EGRET search for high-energy gamma radiation from pulsars similar to those that have already been detected. These are pulsars having periods from 30 ms to several seconds, characteristic ages of less than about 10^7 years, powered by the spin-down of the neutron star. The derived upper limits can be combined with the positive results to study collective properties and compare with pulsar model predictions. Other spin-powered pulsars, the millisecond pulsars, have much shorter periods, much larger characteristic ages, and derived surface magnetic fields about four orders of magnitude smaller than those of the first group. Although the spin-down energies of these two classes are comparable, the physical conditions in the pulsar magnetospheres are sufficiently different that the EGRET results for millisecond pulsars

[1] Code 662, NASA Goddard Space Flight Center, Greenbelt, MD 20771.
[2] Department of Physics, Princeton University, Princeton, NJ 08544.
[3] Max-Planck-Institut für Extraterrestrische Physik, Giessenbachstr D-85748 Garching, Germany.
[4] Present address: Royal Observatory, Edinburgh, Scotland.
[5] W. W. Hansen Experimental Physics Laboratory and Department of Physics, Stanford University, Stanford, CA 94305.
[6] Present address: CITA, University of Toronto, Toronto, ON, Canada M5S 1A7.
[7] Istituto di Fisica dell'Università di Palermo & Istituto di Radioastronomie del CNR, I-40126 Bologna, Italy.
[8] USRA Research Associate.
[9] Australia Telescope National Facility, CSIRO, PO Box 76, Epping, NSW 2121, Australia.
[10] Present address: Research Centre for Theoretical Astrophysics, University of Sydney, NSW 2006, Australia.
[11] Department of Physics, Hampden-Sydney College, Hampden-Sydney, VA 23943.
[12] Department of Physics, University of Manchester, Jodrell Bank, Macclesfield, SK11 9DL, UK.
[13] Compton Observatory Science Support Center, operated by USRA.
[14] Dept. of Physics, Potchefstroom University, Potchefstroom 2520, South Africa.
[15] NAS-NRC Senior Research Associate.
[16] Grumman Aerospace Corporation, Bethpage, NY 11714.

are treated in a companion paper (Fierro et al. 1994). Accretion-powered pulsars are seen primarily as X-ray binaries and are characterized by thermal energy spectra that are not expected to extend into the EGRET energy range; these pulsars will be the subject of later work.

2. THE EGRET OBSERVATIONS

EGRET is the high-energy gamma-ray telescope on the *Compton Observatory*. Descriptions and capabilities of the instrument are given by Hughes et al. (1980), Kanbach et al. (1988), Kanbach (1989), and Thompson et al. (1993). The telescope covers the energy from about 30 MeV to over 20 GeV. EGRET records gamma-ray photons individually as electron-positron pair production events, which are processed automatically (with manual verification) to provide the arrival direction and energy of each photon. The arrival time of each photon is recorded in Universal Coordinated Time (UTC) to an accuracy of better than 100 μs. Because of the very low flux level of the high-energy gamma rays, observing periods are typically 2–3 weeks.

Between 1991 April and 1992 November, EGRET carried out observations which mapped the entire sky, and many parts of the sky have been reexamined since then. The sky coverage is not uniform, having greater exposure in the Galactic anticenter than in any other part of the sky. In addition, sources are observed against a diffuse gamma-ray emission which is strongly peaked toward the Galactic plane. For these reasons, the pulsar search sensitivity is also nonuniform.

3. SUMMARY OF EGRET PULSAR DETECTIONS

Results for the five pulsars detected by EGRET have been published separately (Crab: Nolan et al. 1993; Vela: Kanbach et al. 1994; PSR B1706−44: Thompson et al. 1992; Geminga: Bertsch et al. 1992, Mayer-Hasselwander et al. 1994; PSR B1055−52: Fierro et al. 1993). These papers adopted a variety of presentations and analyses of the data. A summary of these results in a uniform format, Table 1, illustrates some of the issues involved in gamma-ray pulsar studies. The columns of this table are as follows:

1. The common name of the pulsar.
2. The spin period P in seconds.
3. The characteristic (or timing) age $\tau = P/2\dot{P}$ in years, where $\dot{P}$ is the time derivative of the period.
4. The gamma-ray spectral index γ between 100 MeV and 2 GeV, where the photon number spectrum $dJ/dE \sim E^{-\gamma}$ photons cm^{-2} s^{-1} MeV^{-1}. An important qualifier is that this number is the average pulsed spectral index. The three pulsars with the best statistics, the Crab, Vela, and Geminga, all show phase-resolved spectral differences. Within the envelope of the pulsed emission, the Crab spectral index varies from 1.43 ± 0.13 to 3.12 ± 0.52 (Nolan et al. 1993), the Vela index varies from 1.45 ± 0.06 to 2.18 ± 0.06 (Kanbach et al. 1994), and the Geminga variation is from 1.22 ± 0.05 to 1.67 ± 0.23 (Mayer-Hasselwander et al. 1994).
5. The observed energy flux in the range 100 MeV to 5 GeV, assuming the average power law. This flux value is an approximation, because the Vela and Geminga energy spectra deviate from the power law at energies above 2 GeV. The energy flux is time-averaged over the full rotation of the pulsar (some of the EGRET references give instantaneous flux values during the pulsed emission).
6. The assumed distance. The adopted distances for radio pulsars are taken from the Taylor, Manchester, & Lyne (1993) catalog, based in most cases on the Taylor & Cordes (1993) model for converting dispersion measure (DM) to distance. These authors note that distance uncertainties of ±25% should be assumed. Recent analysis (Oberlack et al. 1993) suggests a smaller distance to Vela, perhaps as small as 250 pc. Although the traditional 500 pc distance is used here, the possibility that this is overestimated should be kept in mind. The distance to Geminga, which is not seen in radio, is taken to be 250 pc, based on the X-ray spectrum (Halpern & Ruderman 1993). The uncertainties do not exclude distances between 100 and 400 pc.
7. The calculated gamma-ray luminosity in the 100 MeV to 5 GeV range. The beaming geometry for gamma-ray pulsars is uncertain. The beaming solid angle Ω can be thought of as a combination of the size and shape of the beam, incorporating the duty cycle. The beaming fraction f is the fraction of 4π sr which is swept out by the gamma-ray beam as the neutron star rotates. The luminosity L is given by

$$L = \Omega F_E D^2 = 4\pi f F_E D^2 . \quad (1)$$

This equation is sometimes expressed in terms of a "beaming factor" $b = 1/f$ (e.g., Mayer-Hasselwander et al. 1994). The shape of the pulsar light curve does not define a unique geometry. A pulsar in which the gamma-ray beam is nearly aligned with the neutron star rotation axis could radiate into a very small solid angle (e.g., Sturner & Dermer 1994). A nonaligned geometry (e.g., Cheng, Ho, & Ruderman 1986; Hsu & Arons 1993) would produce a much larger beaming solid angle. Both configurations could in principle produce the same observed light curve. In the absence of any conclusive information, the gamma radiation is assumed to be beamed into 1 sr ($f = 1/4\pi$), so that $L = F_E D^2$.
8. The spin-down luminosity $\dot{E}$, from Taylor et al. (1993).
9. The calculated efficiency for conversion of spin-down energy into high-energy gamma radiation, based on the assumptions discussed above.

Some values of Table 1 differ slightly from those in Table 4 of Fierro et al. (1993) due to improved spectral information. Other aspects of the two tables are the same. The five known

TABLE 1

PULSAR DETECTIONS WITH EGRET

Pulsar	P (s)	τ (yr)	γ	F_E (ergs cm^{-2} s^{-1})	D (kpc)	Luminosity (ergs s^{-1})	$\dot{E}$ (ergs s^{-1})	Efficiency
Crab	0.033	1.3E+03	2.15	1.0E−9	2.00	3.94E+34	4.49E+38	0.00009
Vela	0.089	1.1E+04	1.70	7.1E−9	0.50	1.68E+34	6.95E+36	0.00242
B1706−44	0.102	1.7E+04	1.72	8.3E−10	1.82	2.60E+34	3.39E+36	0.00767
Geminga	0.237	3.4E+05	1.50	3.7E−9	0.25	2.21E+33	3.26E+34	0.06780
B1055−52	0.197	5.3E+05	1.18	4.2E−10	1.53	9.31E+33	3.02E+34	0.30800

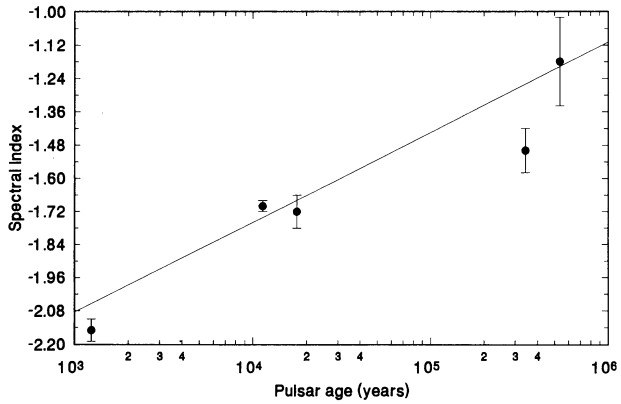

FIG. 1.—Spectral index as a function of characteristic age, for the five detected EGRET pulsars.

pulsars show a clear trend for spectral hardening with pulsar characteristic age τ, as noted by Fierro et al. (1993), and shown in Figure 1. The spectral index γ can be expressed as:

$$\gamma = 0.33 \log \tau - 3.08 \quad (2)$$

with τ in years. Although this line is not a good fit to the data points (χ^2/degree of freedom = 4.1), it provides a useful representation of the observed trend. If the low-energy gamma-ray spectrum of PSR 1509−58 (Wilson et al. 1993; Matz et al. 1994) is assumed to steepen near 1 MeV, then the EGRET upper limits for this pulsar (Brazier et al. 1994) imply that the spectrum between 1 MeV and 5 GeV must be at least as steep as −2.1, consistent with the trend shown in Figure 1.

4. PULSAR SEARCHES

Over 500 spin-powered pulsars are now known (Taylor et al. 1993). Most of these are not expected to be observable as gamma-ray emitters due to their spin-down energy or distance. A measure of the potential visibility of a pulsar is given by $\dot{E}/D^2$, where $\dot{E}$ is the spin-down energy and D is the distance to the pulsar (Taylor 1989). Table 1 shows that the observed gamma radiation from PSR B1055−52 represents ~30% of the $\dot{E}$. This detection achieved a high level of significance only when data from five separate observations were combined (Fierro et al. 1993). Pulsars with lower values of $\dot{E}$ or larger distances would have to convert an even larger fraction of their spin-down energy into gamma rays in order to be observable. Pulsars with significantly lower values of $\dot{E}/D^2$ than that for PSR B1055−52 are, therefore, poor candidates to be visible as gamma-ray pulsars. The present work involves 40 pulsars with values of $\dot{E}/D^2$ down to $\frac{1}{5}$ that of PSR B1055−52, including the two for which EGRET limits have already been published (Brazier et al. 1994).

Searches for gamma-ray pulsars can be carried out in two ways. The first approach looks for pulsations of detected gamma rays at the known radio period. The second method searches the map of the gamma-ray sky for pointlike excesses in the directions of known pulsars, seen above the diffuse gamma radiation. The same photons are analyzed in time and in coordinate space.

The timing analysis uses the same procedures developed for the detected EGRET pulsars (Nolan et al. 1993; Thompson 1993). For each pulsar, gamma rays are chosen from within a cone of radius $\theta \leq 5.^\circ85\,(E_\gamma/100\ \mathrm{MeV})^{-0.534}$, with E_γ in MeV, which reflects the energy-dependent angular resolution of the EGRET instrument (Thompson et al. 1993). After correction of the UTC arrival times to the solar system barycenter, the individual gamma-ray arrival times are folded using the known period P and period derivative $\dot{P}$ as determined from radio observations. The resulting phase plot is examined visually and with a number of statistical tests for nonuniformity: χ^2, Rayleigh, Z_2^2, Z_{10}^2 (Buccheri et al. 1983), and H-test (De Jager, Swanepoel, & Raubenheimer 1989). The H-test offers some advantages over the other tests when searching for an unknown pulse shape in sparse data (De Jager 1994). It is independent of the binning of the data, and it is sensitive to a wide variety of pulse shapes. For these reasons, the H-test (specifically, the probability derived from the H-test that a given set of gamma ray phase values occurs by chance) is used to assess the EGRET results for each candidate pulsar, with the other tests used to verify consistency. The evaluation is made for all photons above 100 MeV and for one or more higher energy thresholds, based on the available statistics.

Some radio pulsars are monitored routinely in radio timing programs; others have been observed regularly as part of a cooperative effort between radio astronomers and the *CGRO* instrument teams (Arzoumanian et al. 1994; Johnston et al. 1994; Kaspi 1993). Continual monitoring of these young pulsars is important, because many of them have significant timing noise or frequent glitches. The reference radio timing information is compiled in the *CGRO* timing database maintained at Princeton University. It should be emphasized that the gamma-ray timing analysis is done only for those observations which have contemporaneous radio timing with enough coverage to provide a unique timing solution. No search of the gamma-ray data for different pulsar periods is undertaken, nor is any such search justified when observing pulsars with well-defined radio timing parameters.

From this analysis, only one new candidate pulsar appeared, PSR B0355+54. The phase plot for gamma rays above 1000 MeV, where the signal is strongest, is shown as Figure 2. This pulsar lies in a region of the sky ($l = 148.^\circ2$, $b = 0.^\circ8$) which has had limited exposure by EGRET, as can be seen by the low statistics. In six viewing periods between 1991 November and 1993 March, the pulsar was always 15° or more from the pointing axis of the instrumment. For the data shown in Figure 2, the H-test indicates a probability of chance occurrence of 0.002 for a single trial. When the number of pulsars (40) and energy selections (two essentially independent energy ranges

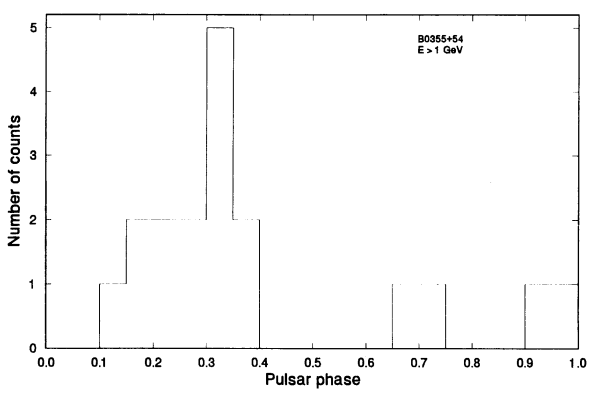

FIG. 2.—Phase plot for the best candidate pulsar, PSR B0355+54, at photon energies above 1 GeV. Considering the number of trials, this is not a statistically significant detection.

for each pulsar) are considered, this is not a significant detection. Nevertheless, the light curve resembles those of PSR B1706−44 and PSR B1055−52, with a broad peak. This pulsar should, therefore, be a prime candidate for future observations.

The second approach to searching for gamma-ray pulsars involves the search of the EGRET data for point sources which are positionally coincident with known pulsars. Like the pulsars, the EGRET gamma-ray sources are concentrated along the Galactic plane. Analysis of the *Compton Observatory* all-sky survey (Fichtel et al. 1994) shows EGRET sources consistent in position with five of the young pulsars: PSR B0611+22, PSR B1046−58, PSR B1356−60, PSR B1758−23, and PSR B1853+01. A possible sixth candidate, PSR B1823−13, lies just outside an EGRET error box in a region where source confusion affects the gamma-ray analysis. A typical EGRET error box, at 95% confidence, subtends about 3 deg^2, and there are 27 unidentified EGRET sources within 2°.5 of the Galactic plane (1800 deg^2). The EGRET error boxes therefore cover 0.045 of the total area. This value represents the probability that any single set of coordinates falls within one of the EGRET error boxes. Of the 40 candidate radio pulsars, 30 lie within 2°.5 of the Galactic plane. The binomial probability that exactly 5 of these 30 radio pulsars fall into EGRET error boxes (i.e., all five which show positional agreement do so by chance) is

$$\frac{30!}{25!5!} \times 0.045^5 \times 0.955^{25} = 0.0083 . \quad (3)$$

The probability of finding 5 or more is 0.010. This probability is too large to claim a positive correlation, although it might suggest that not all five are chance coincidences. It is statistically likely that at least two of the five are chance superpositions. Including the sixth candidate would reduce the probability of all being chance occurrences to 0.002.

None of these six sources near known pulsars shows evidence of pulsed emission. Conversely, the best candidate from the pulsed search, PSR B0355+54, is not detectable as a point source in the spatial analysis.

5. UPPER LIMITS TO PULSAR GAMMA RADIATION

5.1. *Pulsed Emission*

The calculation of pulsed upper limits for gamma-ray pulsars is complicated by the fact that the pulse shape is unknown. Three of the EGRET pulsars (Crab, Vela, Geminga) show two narrow pulses with a bridge of excess emission between them (Nolan et al. 1993; Bertsch et al. 1992; Mayer-Hasselwander et al. 1994; Kanbach et al. 1994). The other two have a broad peak which shows no well-defined structure within present statistics (Thompson et al. 1992; Fierro et al. 1993). Past calculations of upper limits for gamma-ray pulsars have used different methods, including a simple binned phase plot with a χ^2 test (Ögelman et al. 1976), a Z_2^2 test (Buccheri et al. 1983), and a Rayleigh power test (Brazier 1994; Brazier et al. 1994).

The present work is based on a new extension of the H-test (De Jager 1994) that allows upper limits to be determined from the H parameter (which is independent of pulse shape) for a variety of assumed pulse widths. The results from this method have been compared to the binned and Rayleigh power methods, showing general consistency. In order to have conservative upper limits for comparisons with models, we give 3 σ (approximately 99.9% confidence) limits for two possible pulse shapes: a narrow pulse (Gaussian) with a 10% full width half-maximum, and a broad, sinusoidal pulse spanning half the phase. Details of this calculation method are given by De Jager (1994).

5.2. *Unpulsed Emission*

Upper limits for these pulsars as steady gamma-ray sources are based on the spatial analysis of the EGRET data, principally the all-sky survey. In the EGRET energy range, the primary large-scale sources of gamma rays are the diffuse radiation produced by cosmic-ray particles interacting with matter and fields in the Galaxy and an isotropic, presumably extragalactic component. Gamma-ray sources are detected as excesses, distributed as the point spread function of EGRET, against the diffuse emission. The Galactic emission model is described by Bertsch et al. (1983). The analysis was carried out using a maximum likelihood method (Mattox et al. 1994) in an iterative process, starting with a comparison to the diffuse model plus isotropic component, then taking into account detected sources as they were found. Upper limits were then derived for the direction of the candidate pulsars. For consistency with the pulsed limits, these are 3 σ (99.9% confidence) limits (most EGRET results use 95% confidence upper limits).

6. RESULTS

Two sets of results are given for the 40 candidate pulsars. Table 2 covers the energy range above 100 MeV, while Table 3 refers to energies above 1 GeV (1000 MeV). The columns of each table are the following:

1. The pulsar name, ordered by increasing right ascension (the B in the name indicates epoch B1950).
2. The characteristic (or timing) age $\tau = P/2\dot{P}$ in years, where $\dot{P}$ is the time derivative of the period.
3. N, the number of photons selected for this energy range.
4. The probability (in percent) that the gamma-ray arrival times, folded with the pulsar timing solution, represent a random distribution, based on the H-test.
5. The total EGRET exposure to the pulsar, in units of 10^8 cm^2 s.
6. The narrow (10%) pulse 99.9% confidence pulsed flux upper limit. The flux limit is given in units of 10^{-7} photons cm^{-2} s^{-1} above 100 MeV and in units of 10^{-8} photons cm^{-2} s^{-1} above 1000 MeV and is averaged over the full rotation phase.
7. The broad (50%) pulse 99.9% confidence pulsed flux upper limit, with units as for the narrow pulse.
8. The unpulsed 99.9% confidence flux limit, based on the spatial analysis, with units as for the narrow pulse. Entries in this column marked with an asterisk are flux values for EGRET-detected sources that are close enough to the pulsar position that a meaningful upper limit cannot be derived. As discussed above, it is likely that most of these are chance positional coincidences.
9. The gamma-ray spectral index γ between 100 MeV and 2 GeV, where the photon number spectrum $dJ/dE \sim E^{-\gamma}$ photons cm^{-2} s^{-1} MeV^{-1}. The assumed spectral index is derived from equation (2), based on the observed gamma-ray pulsars.

TABLE 2

PULSAR UPPER LIMITS WITH EGRET – $E > 100$ MeV

Pulsar	τ	N	Prob. H-test	Expo. x10^8	Flux (x10^{-7}) Nw	Br	Un	γ	$<E>$	D	Luminosity Limits Nar	Br	Unpul	$\dot{E}$	Efficiency Limits η_{Nw}	η_{Br}	η_{Un}
B0114+58	2.7E+05	794	47.6	5.82	1.5	3.9	2.36	1.3	918	2.12	9.5E+33	2.4E+34	1.5E+34	2.2E+35	0.0431	0.1095	0.0670
B0136+57	4.0E+05	802	15.5	5.94	1.7	4.6	2.75	1.2	979	2.89	2.2E+34	5.7E+34	3.4E+34	2.1E+34	1.0327	2.7244	1.6390
B0355+54	5.6E+05	1559	37.6	8.06	1.6	4.1	3.04	1.2	1034	2.07	1.1E+34	2.8E+34	2.1E+34	4.5E+34	0.2383	0.6109	0.4526
B0450+55	2.3E+06	299	40.4	2.17	2.6	6.6	1.49	1.0	1283	0.78	3.1E+33	7.8E+33	1.8E+33	2.4E+33	1.2936	3.3077	0.7491
B0540+23	4.0E+05	4481	35.5	15.82	1.4	3.6	1.32	1.2	979	3.53	2.6E+34	6.7E+34	2.5E+34	2.1E+34	1.2401	3.1865	1.1737
B0540–69	1.7E+03	540	78.6	10.1	0.6	1.6	1.26	2.0	393	49.40	9.2E+35	2.3E+36	1.8E+36	1.5E+38	0.0062	0.0154	0.0125
B0611+22	8.9E+04	2950	63.5	13.69	1.2	2.9	4.45*	1.4	758	4.72	3.0E+34	7.5E+34	1.1E+35	6.3E+34	0.4778	1.1988	1.8273
B0656+14	1.1E+05	804	83.0	8.72	0.9	2.1	1.16	1.4	787	0.76	6.0E+32	1.5E+33	8.0E+32	3.8E+34	0.0157	0.0390	0.0211
B0740–28	1.6E+05	596	41.3	4.83	1.6	4.2	1.60	1.4	835	1.88	7.3E+33	1.9E+34	7.2E+33	1.4E+35	0.0511	0.1306	0.0503
B0906–49	1.1E+05	2345	58.6	8.65	1.7	4.2	2.02	1.4	788	6.57	8.7E+34	2.2E+35	1.0E+35	4.9E+35	0.1774	0.4466	0.2137
B0950+08	1.7E+07	90	29.7	2.24	1.4	3.7	1.49	0.7	1683	0.13	6.2E+31	1.6E+32	6.5E+31	5.6E+32	0.1112	0.2875	0.1157
B1001–47	2.3E+06	0701	63.1	7.23	1.1	2.7	1.04	1.0	1289	3.44	2.5E+34	6.3E+34	2.4E+34	2.8E+33	8.8577	22.2280	8.5615
B1046–58	2.0E+04	1870	55.9	7.32	1.8	4.5	5.78*	1.7	588	2.98	1.4E+34	3.6E+34	4.6E+34	2.0E+36	0.0071	0.0179	0.0230
B1221–63	6.9E+05	1235	70.2	5.44	1.8	4.6	2.36	1.1	1069	2.29	1.6E+34	3.9E+34	2.0E+34	1.9E+34	0.8142	2.0340	1.0457
B1338–62	1.2E+04	2124	39.4	4.89	3.1	7.8	3.35	1.7	538	8.66	1.9E+35	4.8E+35	2.1E+35	1.4E+36	0.1359	0.3478	0.1490
B1356–60	3.2E+05	2115	85.2	4.63	2.6	6.5	7.44*	1.3	941	5.91	1.3E+35	3.2E+35	3.7E+35	1.2E+35	1.0784	2.6820	3.0843
B1449–64	1.0E+06	1155	15.8	4.28	2.9	7.6	2.47	1.1	1138	1.84	1.7E+34	4.5E+34	1.5E+34	1.9E+34	0.9006	2.3745	0.7722
B1509–58	1.5E+03	1880	34.4	4.84	3.0	7.6	5.50	2.0	389	4.40	3.4E+34	8.8E+34	6.3E+34	1.8E+37	0.0019	0.0049	0.0035
B1607–52	5.6E+05	1351	29.4	2.52	4.9	12.8	3.73	1.2	1033	3.34	8.7E+34	2.2E+35	6.5E+34	3.4E+34	2.5841	6.6848	1.9524
B1610–50	7.4E+03	2472	46.2	5.29	3.0	7.5	3.78	1.8	497	7.26	1.2E+35	3.0E+35	1.5E+35	1.6E+36	0.0754	0.1919	0.0962
B1634–45	5.9E+05	3963	42.4	6.36	3.2	8.1	7.01	1.2	1041	3.83	7.4E+34	1.9E+35	1.6E+35	7.5E+34	0.9811	2.5039	2.1695
B1643–43	3.2E+04	3719	55.4	6.78	2.7	6.9	4.87	1.6	637	6.85	1.2E+35	3.1E+35	2.2E+35	3.6E+35	0.3461	0.8734	0.6171
B1702–19	1.1E+06	1035	85.1	8.82	1.0	2.4	1.13	1.1	1157	1.19	2.4E+33	5.9E+33	2.8E+33	6.1E+33	0.3899	0.9697	0.4609
B1719–37	3.5E+05	4706	26.8	8.14	2.9	7.5	3.02	1.2	954	2.52	2.7E+34	6.9E+34	2.8E+34	3.2E+34	0.8231	2.1360	0.8612
B1727–33	2.6E+04	4952	94.2	8.72	2.1	5.1	3.00	1.6	613	4.24	3.5E+34	8.6E+34	5.0E+34	1.2E+36	0.0280	0.0697	0.0407
B1737–30	2.1E+04	5987	63.4	9.22	2.5	6.2	3.25	1.7	589	3.28	2.4E+34	6.0E+34	3.1E+34	8.2E+34	0.2885	0.7238	0.3807
B1754–24	2.9E+05	5242	33.0	7.78	3.1	8.0	3.37	1.3	925	3.50	5.4E+34	1.4E+35	5.8E+34	4.0E+34	1.3480	3.4729	1.4652
B1757–24	1.5E+04	5495	81.5	9.30	2.1	5.3	2.82	1.7	561	4.61	3.9E+34	9.7E+34	5.1E+34	2.6E+36	0.0149	0.0372	0.0197
B1758–23	5.8E+04	2328	63.6	3.29	4.3	10.8	7.03*	1.5	704	3.00	4.2E+34	1.0E+35	6.8E+34	6.2E+34	0.6688	1.6777	1.0935
B1800–21	1.6E+04	5563	20.4	9.18	2.9	7.5	4.74	1.7	563	3.94	3.8E+34	1.0E+35	6.3E+34	2.2E+36	0.0172	0.0451	0.0285
B1822–09	2.3E+05	6126	74.7	8.86	2.5	6.1	3.82	1.3	893	1.03	3.5E+33	8.8E+33	5.5E+33	4.6E+33	0.7792	1.9419	1.2110
B1823–13	2.1E+04	6866	53.1	9.10	2.8	7.1	4.07	1.6	593	4.12	4.3E+34	1.1E+35	6.2E+34	2.8E+36	0.0151	0.0382	0.0220
B1828–10	1.1E+05	6270	34.9	8.65	3.0	7.8	2.96	1.4	782	3.63	4.7E+34	1.2E+35	4.6E+34	3.6E+34	1.3291	3.4174	1.3006
B1830–08	1.5E+05	5589	99.9	8.93	2.1	5.3	3.53	1.4	826	5.67	8.7E+34	2.2E+35	1.4E+35	5.8E+35	0.1482	0.3693	0.2446
B1853+01	2.0E+04	4289	25.1	8.30	2.7	7.1	7.02*	1.7	588	3.30	2.7E+34	6.9E+34	6.8E+34	4.3E+35	0.0619	0.1609	0.1594
B1915+13	4.3E+05	3573	82.2	7.30	2.2	5.4	2.85	1.2	988	4.07	5.5E+34	1.4E+35	7.1E+34	3.9E+34	1.4134	3.5146	1.84232
B1929+10	3.1E+06	2141	31.7	7.50	2.1	5.3	1.63	0.9	1342	0.17	1.2E+32	3.2E+32	9.6E+31	3.9E+33	0.0310	0.0799	0.0244
B1930+22	4.0E+04	2953	40.9	9.75	1.8	4.6	3.60	1.6	659	9.80	1.7E+35	4.4E+35	3.5E+35	7.5E+35	0.2296	0.5867	0.4601
B1951+32	1.1E+05	2939	55.7	11.6	1.4	3.6	2.77	1.4	782	2.50	1.1E+34	2.7E+34	2.1E+34	3.7E+36	0.0028	0.0071	0.0055
B2334+61	4.1E+04	886	48.3	4.50	2.1	5.2	4.10	1.6	662	2.46	1.3E+34	3.2E+34	2.5E+34	6.2E+34	0.2023	0.5136	0.4011

* Unpulsed flux of EGRET source consistent in position with this pulsar.

10. The average photon energy for this spectral index, in MeV, for the energy range.

11. The assumed distance to the pulsar, in kpc. The adopted distance is taken from the Taylor et al. (1993) catalog, based in most cases on the Taylor & Cordes (1993) model. These authors note that distance uncertainties of at least $\pm 25\%$ should be assumed. The one exception to the use of these distance estimates is PSR B1758−23. The distance estimated from the DM is 13.5 kpc (Kaspi et al. 1993). We adopt instead the distance estimate of 3 kpc by Frail, Kulkarni, & Vasisht (1993), who associate the pulsar with the supernova remnant W28 and identify the large DM as resulting from a dense screen of ionized material along the line of sight.

12. The narrow pulse luminosity upper limit in ergs s^{-1}, assuming a beaming solid angle of 1 sr.

13. The broad pulse luminosity upper limit in ergs s^{-1}, assuming a beaming solid angle of 1 sr.

14. The unpulsed luminosity upper limit in ergs s^{-1}, assuming a beaming solid angle of 1 sr.

15. $\dot{E}$ in ergs s^{-1}, from Taylor et al. (1993).

16. The gamma-ray production efficiency upper limit η for a narrow pulse (narrow pulse luminosity limit/$\dot{E}$). Values of η greater than 1.0, which would be nonphysical, are shown to illustrate the full range for the particular assumptions used in this calculation. In light of the uncertainties in beaming fraction and distance, nominal values of η above 1.0 cannot be excluded.

17. The gamma-ray production efficiency upper limit for a broad pulse.

18. The gamma-ray production efficiency upper limit for unpulsed emission.

Tables 2 and 3 show that the PSR B0355+54, with a single trial probability of chance occurrence of 0.2%, is the only candidate for pulsed emission. As noted above, the number of pulsars and energies tested is large enough that no claim of a positive result is justified for PSR B0355+54. None of the other calculated probabilities of chance occurrence fall below 7% above 1000 MeV and none fall below 15% for the $E > 100$ MeV sample. The only one of the unpulsed sources near known pulsars which shows any hint of pulsation is PSR B1046−58, with a 14% probability of chance occurrence above 1000 MeV.

Table 2 shows that in most cases the unpulsed upper limit lies between the limits derived from the two assumptions about pulse shape for the energy range above 100 MeV. In a few cases, the unpulsed limit is more restrictive than either of the pulsed limits. For those pulsars which lie close to detected EGRET sources (within 1°), the flux from the source may exceed the pulsed limits. If the EGRET source were subtracted

TABLE 3

PULSAR UPPER LIMITS WITH EGRET – $E > 1000$ MeV

Pulsar	τ	N	Prob. H-test	Expo. x10^8	Flux (x10^{-8}) Nw	Br	Un	γ	< E >	D	Luminosity Limits Nar	Br	Unpul	$\dot{E}$	Efficiency Limits η_{Nw}	η_{Br}	η_{Un}
B0114+58	2.7E+05	8	15.7	4.18	2.5	6.5	4.0	1.3	2343	2.12	3.9E+33	1.0E+34	2.5E+34	2.2E+35	0.0178	0.0469	0.1136
B0136+57	4.0E+05	12	46.4	4.40	2.5	6.3	3.7	1.2	2370	2.89	7.5E+33	1.9E+34	4.6E+34	2.1E+34	0.3580	0.9094	2.2051
B0355+54	5.6E+05	18	0.2	5.50	3.6	10.1	2.4	1.2	2395	2.07	5.6E+33	1.6E+34	1.6E+34	4.5E+34	0.1226	0.3494	0.3573
B0450+55	2.3E+06	4	44.2	1.39	4.6	11.7	2.4	1.0	2497	0.78	1.1E+33	2.7E+33	2.9E+33	2.4E+33	0.4474	1.1387	1.2065
B0540+23	4.0E+05	48	48.9	11.56	1.9	4.7	3.1	1.2	2370	3.53	8.4E+33	2.1E+34	5.8E+34	2.1E+34	0.4025	1.0202	2.7565
B0540−69	1.7E+03	8	81.7	8.83	0.9	2.1	2.3	2.0	2005	49.40	6.4E+35	1.6E+36	3.4E+36	1.5E+38	0.0043	0.0107	0.0227
B0611+22	8.9E+04	59	87.0	10.18	2.0	4.9	3.1*	1.4	2263	4.72	1.5E+34	3.7E+34	8.0E+34	6.3E+34	0.2394	0.5951	1.2730
B0656+14	1.1E+05	4	46.7	5.82	1.1	2.7	1.2	1.4	2279	0.76	2.2E+32	5.5E+32	8.3E+32	3.8E+34	0.0057	0.0145	0.0218
B0740−28	1.6E+05	5	58.3	3.20	2.1	5.3	4.7	1.4	2303	1.88	2.6E+33	6.5E+33	2.1E+34	1.4E+35	0.0182	0.0457	0.1478
B0906−49	1.1E+05	37	68.6	6.41	2.7	6.8	3.0	1.4	2279	6.57	4.1E+34	1.0E+35	1.6E+35	4.9E+35	0.0832	0.2078	0.3173
B0950+08	1.7E+07	1	45.1	1.49	2.1	5.4	3.8	0.7	2650	0.13	1.5E+31	3.7E+31	1.6E+32	5.6E+32	0.0260	0.0661	0.2951
B1001−47	2.3E+06	4	17.2	5.24	1.4	3.6	1.7	1.0	2500	3.44	6.2E+33	1.6E+34	4.0E+34	2.8E+33	2.1914	5.7582	13.9947
B1046−58	2.0E+04	44	13.6	5.27	4.6	12.3	3.1*	1.7	2163	2.98	1.4E+34	3.6E+34	2.5E+34	2.0E+36	0.0068	0.0179	0.0123
B1221−63	6.9E+05	18	28.6	3.57	4.0	10.5	4.4	1.1	2410	2.29	7.8E+33	2.0E+34	3.8E+34	1.9E+34	0.4033	1.0431	1.9496
B1338−62	1.2E+04	37	24.4	3.50	6.0	15.7	5.3	1.7	2129	8.66	1.5E+35	3.8E+35	3.3E+35	1.4E+36	0.1058	0.2752	0.2357
B1356−60	3.2E+05	39	72.1	3.30	5.3	13.3	9.7	1.3	2353	5.91	6.7E+34	1.7E+35	4.9E+35	1.2E+35	0.5529	1.3782	4.0212
B1449−64	1.0E+06	9	89.2	3.09	2.5	6.2	4.4	1.1	2439	1.84	3.1E+33	7.8E+33	2.6E+34	1.9E+34	0.1661	0.4134	1.3755
B1509−58	1.5E+03	39	85.3	3.51	4.7	11.6	6.3	2.0	2001	4.40	2.7E+34	6.8E+34	7.2E+34	1.8E+37	0.0015	0.0038	0.0040
B1607−52	5.6E+05	36	82.2	1.89	8.5	21.1	6.8	1.2	2394	3.34	3.4E+34	8.6E+34	1.2E+35	3.4E+34	1.0281	2.5537	3.5593
B1610−50	7.4E+03	62	77.7	3.85	5.6	13.9	4.8	1.8	2098	7.26	9.4E+34	2.3E+35	1.9E+35	1.6E+36	0.0602	0.1497	0.1222
B1634−45	5.9E+05	99	81.1	4.46	6.0	14.9	10.4	1.2	2398	3.83	3.2E+34	8.0E+34	2.4E+35	7.5E+34	0.4271	1.0610	3.2187
B1643−43	3.2E+04	61	67.0	4.73	4.8	11.9	8.6	1.6	2194	6.85	7.5E+34	1.9E+35	3.9E+35	3.6E+35	0.2082	0.5205	1.0898
B1702−19	1.1E+06	8	40.6	6.50	1.4	3.6	1.9	1.1	2446	1.19	7.4E+32	1.9E+33	4.7E+33	6.1E+33	0.1211	0.3093	0.7750
B1719−37	3.5E+05	81	7.9	5.96	5.8	15.6	4.5	1.2	2359	2.52	1.3E+34	3.6E+34	4.2E+34	3.2E+34	0.4092	1.0968	1.2832
B1727−33	2.6E+04	115	81.2	6.31	4.6	11.3	5.3	1.6	2179	4.24	2.7E+34	6.8E+34	8.9E+34	1.2E+36	0.0220	0.0547	0.0719
B1737−30	2.1E+04	164	8.7	6.60	7.4	19.8	5.0	1.7	2164	3.28	2.6E+34	7.0E+34	4.8E+34	8.2E+34	0.3186	0.8520	0.5858
B1754−24	2.9E+05	142	25.8	5.60	7.3	19.0	9.9	1.3	2346	3.50	3.2E+34	8.3E+34	1.7E+35	4.0E+34	0.8073	2.0953	4.3043
B1757−24	1.5E+04	118	98.7	6.70	4.1	10.3	4.9	1.7	2145	4.61	2.9E+34	7.2E+34	8.9E+34	2.6E+36	0.0111	0.0276	0.0343
B1758−23	5.8E+04	61	44.8	0.84	29.5	75.1	8.3	1.5	2234	3.00	9.0E+34	2.3E+35	8.0E+34	6.2E+34	1.4546	3.7004	1.2910
B1800−21	1.6E+04	136	68.1	6.60	5.1	12.7	6.2	1.7	2146	3.94	2.6E+34	6.4E+34	8.3E+34	2.2E+36	0.0116	0.0290	0.0372
B1822−09	2.3E+05	83	23.6	6.08	5.2	13.6	7.1	1.3	2331	1.03	2.0E+33	5.1E+33	1.0E+34	4.6E+33	0.4313	1.1228	2.2509
B1823−13	2.1E+04	138	17.0	6.20	6.8	18.0	8.7	1.6	2167	4.12	3.8E+34	1.0E+35	1.3E+35	2.8E+36	0.0135	0.0355	0.0471
B1828−10	1.1E+05	95	38.8	5.90	5.4	13.8	4.3	1.4	2276	3.63	2.5E+34	6.3E+34	6.7E+34	3.6E+34	0.6868	1.7571	1.8894
B1830−08	1.5E+05	133	44.7	6.29	5.8	14.8	4.6	1.4	2299	5.67	6.5E+34	1.7E+35	1.9E+35	5.8E+35	0.1121	0.2853	0.3188
B1853+01	2.0E+04	116	37.7	6.00	5.9	15.0	9.4	1.7	2163	3.30	2.1E+34	5.4E+34	9.2E+34	4.3E+35	0.0490	0.1254	0.2134
B1915+13	4.3E+05	54	74.9	5.35	3.8	9.5	4.0	1.2	2375	4.07	2.3E+34	5.7E+34	1.0E+35	3.9E+34	0.5931	1.4765	2.5869
B1929+10	3.1E+06	12	13.8	5.58	2.3	6.0	1.7	0.9	2520	0.17	2.5E+31	6.7E+31	1.0E+32	3.9E+33	0.0064	0.0170	0.0255
B1930+22	4.0E+04	45	39.5	6.70	3.2	8.3	3.6	1.6	2208	9.80	1.0E+35	2.7E+35	3.5E+35	7.5E+35	0.1389	0.3551	0.4601
B1951+32	1.1E+05	53	28.2	8.65	2.9	7.4	4.4	1.4	2276	2.50	6.2E+33	1.6E+34	3.3E+34	3.7E+36	0.0017	0.0043	0.0088
B2334+61	4.1E+04	10	96.1	3.35	2.4	6.0	7.6	1.6	2210	2.46	4.9E+33	1.2E+34	4.6E+34	6.2E+34	0.0787	0.1959	0.7436

* Unpulsed flux of EGRET source consistent in position with this pulsar.

from the map, the residual unpulsed upper limits would be lower. Because the EGRET point-spread function is too broad to allow easy separation of sources separated by less than 1°, the detected flux can be considered a conservative upper limit to a second source nearby.

The comparison of the various efficiency upper limits for the $E > 100$ MeV energy range is shown in Figure 3, where the limits are presented as a function of pulsar characteristic age. The narrow (triangle pointed up) and broad (triangle pointed down) pulsed limits are connected with a line, while the unpulsed limit is shown as a circle. The unpulsed limits do not depend on the pulse shape, although they do depend on the model for the diffuse radiation. The fact that the two pulsed limits generally bracket the unpulsed limit indicates that these different approaches to analysis (time and space) are complementary and produce compatible results. The five unpulsed source detections which are positionally coincident with radio pulsars are shown as filled squares, assuming the distance to the pulsar and the same 1 sr beaming as used for the pulsed luminosity calculation. It should be noted that the efficiency (which depends on $\dot{E}$) and the characteristic age τ are not strictly independent, because both are derived from the pulsar P and $\dot{P}$.

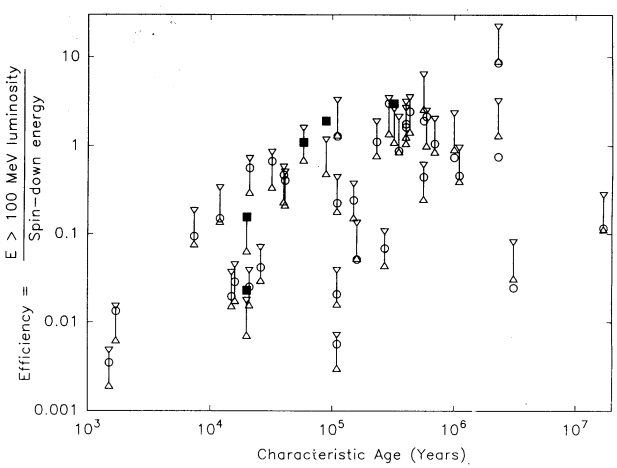

FIG. 3.—Efficiency for conversion of pulsar spin-down energy into high-energy gamma radiation (100–5000 MeV), assuming a beaming solid angle of 1 sr. *Triangles pointed down*: pulsed limit assuming a broad pulse; *triangles pointed up*: pulsed limit assuming a narrow pulse; *open circles*: unpulsed limit; *filled squares*: unpulsed luminosity for sources positionally coincident with known pulsars, expressed as a fraction of the spin-down energy, assuming the source is at the pulsar distance.

7. DISCUSSION

7.1. *Gamma-Ray Pulsar Detections and Upper Limits*

Comparison of the efficiency upper limits (Table 2 and Fig. 3) with the results for the five detected pulsars (Table 1) is shown in Figure 4. The unpulsed upper limits for conversion efficiency (open circles) are shown as a function of pulsar characteristic age, along with the unpulsed efficiencies for the sources positionally coincident with radio pulsars (solid squares) and the efficiencies for the EGRET-detected pulsars (solid circles). The error bars shown for the detected pulsars are based on the distance uncertainties. The trend for increasing efficiency with characteristic age was first suggested by Buccheri et al. (1978). With τ in years, the line can be represented as

$$\eta = 3.6 \times 10^{-8} \tau^{1.17} . \quad (4)$$

Based solely on the detected pulsars, this trend could be a selection effect, with the older pulsars only being detectable if their efficiency is high. What the upper limits add is the fact that none of the young pulsars have high efficiencies for high-energy gamma-ray production. Ten additional pulsars with $\tau < 3 \times 10^4$ yr would have been visible to EGRET if their efficiencies were as high as that of PSR B1055−52.

A few of the upper limits for older pulsars lie more than an order of magnitude below the line represented by equation (4), indicating that the simple observed trend does not hold for all pulsars. The upper limits do not rule out the possibility that the typical gamma-ray efficiency of pulsars is low with the two exceptions being ones with larger values of τ.

7.2. *Gamma-Ray Pulsar Models*

Harding (1981) modeled the gamma-ray efficiency based on the polar cap cascade concept, described in detail by Daugherty & Harding (1982). In this model, the quantity $\eta \dot{P}^{-1.3}$ is expected to be proportional to $\tau^{1.8}$. Figure 5 shows that the five detected pulsars (shown as solid dots) are consistent with this trend, although the best-fit line (solid) is steeper than $\tau^{1.8}$. The energy range of EGRET does not, however, encompass the full gamma-ray luminosity of these pulsars (see Nel & De Jager 1994 for a summary of the broad-band spectra of these pulsars). Particularly for the Crab, with its steeper spectrum, the maximum luminosity lies close to 100 keV photon energy. Integrating the spectra of the detected pulsars from 100 keV to 5000 MeV produces the points shown as X in Figure 5. The fit to these points (dashed line) does have a slope of approximately $\tau^{1.8}$. A few of the upper limits fall well below the line, suggesting that beaming or other factors besides the characteristic age influence the gamma-ray production efficiency. This model makes no specific prediction about efficiencies for older pulsars, where the line would predict an efficiency greater than 100%.

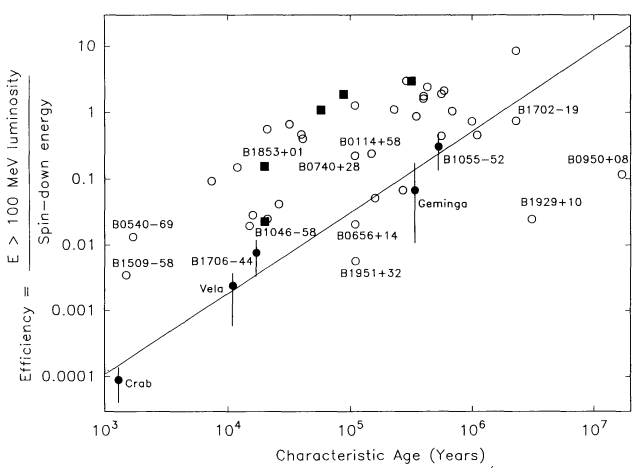

FIG. 4.—Efficiency for conversion of pulsar spin-down energy into high-energy gamma radiation (100–5000 MeV), assuming a beaming solid angle of 1 sr. *Open circles*: unpulsed upper limits; *filled squares*: unpulsed luminosity for sources positionally coincident with known pulsars, expressed as a fraction of the spin-down energy, assuming the source is at the pulsar distance; *filled circles*: efficiencies for detected pulsars; *solid line*: fit to the efficiencies for detected pulsars. The error bars shown for the detected pulsars are based on the distance uncertainties, including the possibility that Vela is closer than the standard 0.5 kpc distance.

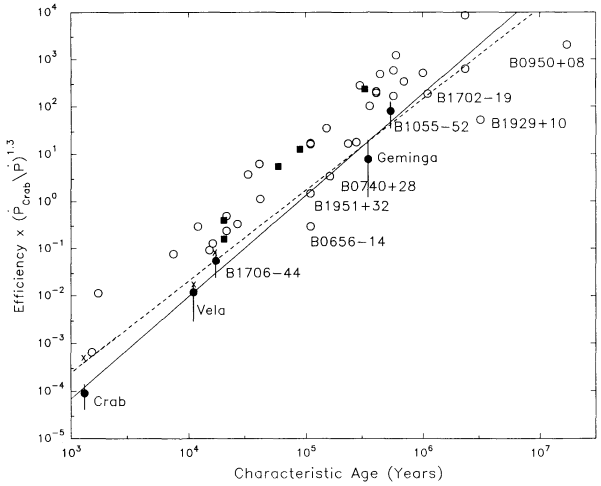

FIG. 5.—*Open circles*: upper limits to gamma-ray efficiency as a function of characteristic age, scaled according to the polar cap model. *Filled circles*: detected pulsars. *Solid line*: fit to these points. *X*: detected pulsars adding the portion of the observed spectrum from 100 keV–100 MeV. *Dashed line*: fit to these points.

The outer gap model (Cheng et al. 1986; Ruderman & Cheng 1988; Chen & Ruderman 1993) predicts that the gamma-ray production efficiency is a function of the pulsar period, characteristic age, and angle between the stellar spin and dipole magnetic field axes. Beyond a "death line," the gamma-ray luminosity should drop quickly as the outer gap is quenched. This model is illustrated in Figure 6, which plots the period and surface magnetic fields for the EGRET-detected pulsars and those from Table 2 that have 99% upper limits to efficiency less than 20%. The line marked "D" is (Chen & Ruderman 1993):

$$5 \log B - 12 \log P = 69.5 \quad (5)$$

with B in Gauss and P in seconds.

Pulsars near this line, such as Geminga and PSR B1055−52, should convert a large fraction of their spin-down energy into gamma radiation. The only new pulsar candidate in this study, PSR B0355+54, does lie close to this line. However, from Tables 2 and 3, EGRET limits on PSRs B0656+14, B0740−28, and B1853+01 imply that they do not show such a high efficiency, even though they lie close to the line. Pulsars to the left of the line should have efficiencies comparable to Vela and PSR B1706−44, with even lower efficiencies expected for Crab-type pulsars such as PSR B0540−69. The EGRET upper limits to the conversion efficiency for pulsars B1509−58

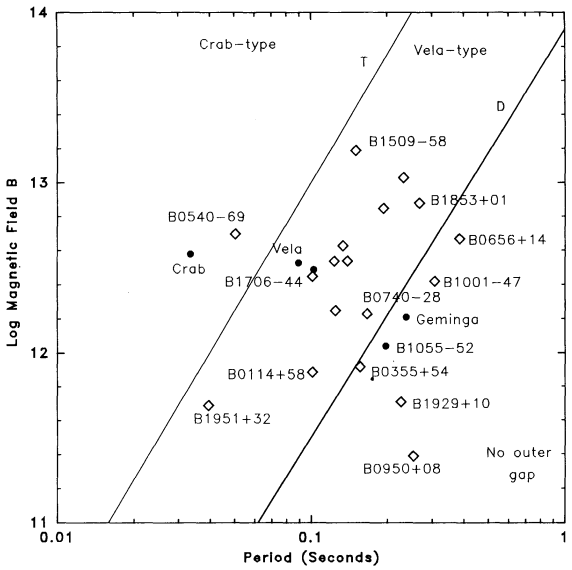

FIG. 6.—Pulsar periods vs. magnetic fields, for the EGRET-detected pulsars (*filled circles*) and others from Table 1 that have efficiency upper limits less than 20% (*open diamonds*). Pulsars of particular interest are identified. The line marked "D" is the death line for an outer magnetosphere accelerator; the line marked "T" is the transition line between Crab-like and Vela-like outer magnetosphere accelerators (Chen & Ruderman 1993).

and B1951+32 are comparable to or below the efficiencies for Vela and PSR B1706−44 (see Fig. 4). Although none of these upper limits strongly contradicts the proposed model, they do indicate that its predictive power is limited in its present form.

Other pulsar models, such as those of Sturner & Dermer (1994) and Hsu & Arons (1993), also predict gamma-ray observability of several known pulsars. PSRs B0656+14 and B1951+32 are suggested as likely candidates by both models, as well as the two models discussed above. Understanding why these pulsars are not seen as high-energy gamma-ray sources appears to be a challenge to most theoretical models.

7.3. *Energy Spectra and Beaming*

One of the central questions raised by this study is "Why does EGRET not see more pulsars?" In the case of PSR B1509−58, the answer appears to be that there is a change in the spectrum (Brazier et al. 1994), steepening between the BATSE/OSSE energy ranges and the EGRET energy range. The Crab pulsar also shows a steepening in its energy spectrum in the 100 keV energy range (Ulmer 1994). The Vela pulsar energy spectrum must also be flatter in the energy range below that of EGRET (Kanbach et al. 1994; Bennett et al. 1993). Particularly if additional pulsars are detected in low-energy gamma rays, this answer may explain why some of these others are not seen by EGRET. This would place additional emphasis on modeling of gamma-ray pulsar spectra (e.g., Ho 1993; Sturner & Dermer 1994; Daugherty & Harding 1994). Unless the energy spectra of Vela, PSR B1706−44, Geminga, and PSR B1055−52 are atypical of young pulsars, however, the trend shown in Figure 1 implies that their luminosity is strongly dominated by their high-energy radiation.

A significant uncertainty in the absolute value for the luminosity of a gamma-ray pulsar arises from the unknown beaming geometry. Helfand (1994) argues (persuasively) that the statistics of gamma-ray pulsar detections imply that at least some beaming fractions must be larger than the $f = 1/4\pi$ used in the tables. On the other hand, a significantly larger value of f for PSR B1055−52 could lead to a nonphysical situation in which more than 100% of the spin-down energy appears to be transformed into high-energy gamma radiation (the lower limit of 0.20 suggested by Helfand would raise the gamma-ray production efficiency to about 75%). What seems likely is that the beaming fraction is not the same for all gamma-ray pulsars. In the radio, a trend toward narrower beams for longer period pulsars has been interpreted as an angular pulse width that varies as $P^{-0.5}$ (Rankin 1990) or $P^{-0.33}$ (Lyne & Manchester 1988), with some additional effect of the angle between the magnetic and rotation axes of the neutron star. If the same sort of relationship applies to these gamma-ray pulsars (as suggested, for example, by Harding & Daugherty 1993, and Dermer & Sturner 1994), then the beaming solid angle for the Crab could be several times larger than that of PSR B1055−52. Notice, however, that the calculated efficiency differs by a factor of more than 3000 for these two pulsars, so the difference due to beaming seems unlikely to account for more than a small part of the total. Nevertheless, the assumption of a constant beaming fraction must be acknowledged as a significant approximation.

For many of the younger radio pulsars, the EGRET upper limits do not constrain the possibility that they are gamma-ray pulsars at a level below the EGRET sensitivity. If some distinguishing features can be found for the several that are expected but not seen, then the remainder could be attributed to sensitivity limitation. Helfand (1994), for example suggests that PSRs B0950+08 and B1929+10 appear on candidate lists primarily because they are nearby, while their ages, periods, and X-ray luminosities all suggest that they are unlikely to be gamma-ray luminous.

Radio emission geometry may provide a distinguishing feature for gamma-ray pulsars. Lyne & Manchester (1988) summarize information about radio beam shapes based on polarization measurements. The Crab and Vela pulsars are both orthogonal rotators, with α, the angle between the rotation axis and the magnetic axis, close to 90°. For PSR B1055−52, Lyne & Manchester give $\alpha = 17.^{\circ}9$ in their Table 1, but later give $\alpha = 75°$ (their Table 6) when the analysis includes both the pulse and interpulse. Rankin (1990) finds $\alpha \sim 90°$ for this pulsar. Again, a nearly orthogonal rotator is suggested. Unpublished polarization measurements for PSR B1706−44 indicate that it is not an aligned rotator, although α has not yet been determined. By contrast, some of the pulsars which might be expected according to models to be gamma-ray emitters may have a closer alignment between the magnetic and rotation axes. PSR B0656+14 has $\alpha = 8.^{\circ}2$ (Lyne & Manchester 1988) or $\alpha = 30°$ (Rankin 1990); PSR B0950+08 has $\alpha = 5.^{\circ}9$ (Lyne & Manchester 1988). PSR 1929+10 does not give a clear solution, with possibilities from $\alpha = 6.^{\circ}0$ (Lyne & Manchester 1988) to $\alpha = 90°$ (Rankin 1990). Polarization measurements for PSR B1951+32, unavailable as far as we know, would be of great interest. The radio polarization measurements, which suggest that at least the Crab and Vela are orthogonal rotators, appear difficult to reconcile with nearly aligned rotator models for gamma-ray pulsars such as those of Sturner & Dermer (1994) and Daugherty & Harding (1994). Chiang & Romani (1992), and Romani & Yadigaroglu (1994) indicate that an outer gap model can explain many of the radio polarization and gamma-ray pulsar beaming properties. Nevertheless, the uncertainties in the determination of alignment angles from radio polarization (Miller & Hamilton 1993) leave this argument inconclusive.

The relative phase of the radio and gamma-ray pulses is an important diagnostic for the emission processes. All of the known gamma-ray emitters have a gamma-ray pulse profile which is or may be double, suggesting a hollow-cone beam geometry. We take the midpoint of the two components, or the pulse centroid for PSR B1706−44 where the components are not well resolved, as the gamma-ray reference phase. For the Crab pulsar, we take the radio precursor pulse as defining the radio phase (cf. Smith 1986). The radio pulse then leads the gamma-ray pulse by 0.26, 0.34, and 0.37 periods for the Crab and Vela pulsars and PSR B1706−44, respectively, establishing a trend for increasing phase difference with increasing pulsar period. From the profiles given by Fierro et al. (1993), PSR B1055−52 seems to violate this trend. However, radio polarization measurements (Lyne & Manchester 1988) show that the impact parameter (minimum angle between the observer's line of sight and the magnetic axis) is much smaller for the second and slightly weaker pulse than it is for the stronger pulse. Therefore the second pulse, usually identified as the interpulse, really should be considered the main pulse. Wide variations are observed in the emission intensity across pulsar beams and the two pulses are in any case comparable in strength. For other "interpulse" pulsars, the main pulse has the smaller impact parameter. Lyne & Manchester further show that beam center is at the phase of the trailing hump of the second pulse. Taking this to be the radio reference phase, the radio pulse leads the centroid of the gamma-ray pulse by 0.42 periods. This phase difference is consistent with the trend found for the other three pulsars.

In principle, this pattern can be used to gain confidence in marginal detections. For PSR B0355+54, with a characteristic age similar to that of PSR B1055−52, the radio pulse appears to lead the possible gamma-ray pulse by 0.25 ± 0.10, a somewhat smaller value than the trend would predict. PSR B1046−58, with a characteristic age similar to that of PSR B1706−44, shows an H-test value corresponding to 14% probability of chance occurrence at energies above 1000 MeV, far too large to consider this a detection. Nevertheless, the two small peaks in the light curve are centered on phase 0.32 ± 0.05, consistent with the trend suggested above. None of the other pulsar gamma-ray light curves have sufficiently well defined peaks to test this hypothesis further.

Other possible relationships involving the radio/gamma-ray phases are given by Ulmer (1994) and Romani & Yadigaroglu (1994).

7.4. *Unpulsed Sources near Pulsars and Radio-quiet Gamma-Ray Pulsars*

The positional agreement between five (or six) unpulsed EGRET sources and radio pulsars is not compelling evidence that any of them are actually powered by the rotating neutron stars. Nevertheless, the results in Table 2 can be used to consider the implications of a possible association. For two of the five, the observed flux implies a gamma-ray luminosity a factor of about two greater than $\dot{E}$: PSR B0611+22 and PSR B1356−60. Even allowing for some uncertainty in distance and beaming fraction, these pulsars seem unlikely to be the source of the gamma radiation. PSR B1758−23 has a gamma-ray luminosity comparable to $\dot{E}$. Within uncertainties, the energetics do not exclude the pulsar as a source of gamma radiation. For the other two, PSR B1046−58 and PSR B1853+01, the observed gamma radiation represents a small fraction of the spin-down energy, about 2% in the case of PSR B1046−58. The sixth candidate EGRET source, near PSR B1823−13, has a flux that represents 4% of the spin-down luminosity. Despite the absence of observable pulsation at gamma-ray energies, at least the energetics make these pulsars possible as the origin of the gamma radiation.

Apparently unpulsed gamma radiation from a rotating neutron star could be produced in a nearly aligned rotator model, such as those of Sturner & Dermer (1994) or Daugherty & Harding (1994). In this case, the Earth could always lie within the beam, so that no pulsation would be visible.

A related issue is the question of whether other gamma-ray pulsars are like Geminga in having no observable radio emission, a possibility suggested by many authors following the discovery of a mumber of unidentified gamma-ray sources by *COS B* (see Helfand 1994 for a recent discussion). Finding a Geminga-like pulsation in a high-energy gamma-ray source is difficult without the benefit of knowing at least an approximate period a priori, due to the low count rates (the Crab pulsar rotates an average of 18,000 times between detected EGRET photons). Although techniques are available to search sparse data for periodicities (e.g., Buccheri, Özel, & Sacco 1987; Middleditch, Deich, & Kulkarni 1993), the relatively large error boxes for the gamma-ray sources and the high diffuse radiation along the Galactic plane complicate the procedure. Geminga, although unlikely to be the only source of its kind, may occupy a unique niche in the gamma-ray sky: it is a very bright source in a relatively isolated region of the sky, and it has a single unusual X-ray candidate in its error box. These factors made the search for pulsation far more feasible than for any of the other unidentified gamma-ray sources.

7.5. *Conclusion*

Some remaining challenges for gamma-ray pulsar models are

1. Explanation of the absence of additional high-energy pulsars, perhaps by inclusion of beaming geometry details.
2. Interpretation of the spectral flattening as a function of characteristic age and the sharp high-energy cutoff seen in some gamma-ray pulsars.
3. Determination of geometries which accommodate the range of pulse shapes seen in the EGRET pulsars.
4. Extension of the spectral studies to lower energies, especially in relation to those gamma-ray pulsars that are also X-ray pulsars and those that show spectral breaks at low energies.

Further EGRET work concerning pulsars will include

1. Continuing studies of the known pulsars, addressing questions of spectral details, pulse shapes, and time variability.
2. Adding more observations to the total, in order to continue searches for pulsars and lower the upper limits on those not seen.

The EGRET team gratefully acknowledges support from the following: Bundesministerium für Forschung und Technologie, grant 50 QV 9095 (MPE authors); NASA grant NAG5-1742 (HSC); NASA grant NAG5-1605 (SU); and NASA contract NAS5-31210 (GAC). We thank O. C. De Jager for helpful discussions of upper limit calculations and M. P. Ulmer for a number of useful suggestions.

REFERENCES

Arzoumanian, Z., Nice, D. J., Taylor, J. H., & Thorsett, S. E. 1994, ApJ, 422, 671
Bailes, M., & Kniffen, D. A. 1992, ApJ, 391, 659
Bennett, K., et al. 1993, in Proc. 23rd Int. Cosmic Ray Conf. (Calgary), 1, 172
Bertsch, D. L., et al. 1992, Nature, 357, 306
Bertsch, D. L., Dame, T. M., Fichtel, C. E., Hunter, S. D., Sreekumar, P., Stacy, J. G., & Thaddeus, P. 1993, ApJ, 416, 587
Bignami, G. F., & Caraveo, P. A. 1992, Nature, 357, 287
Brazier, K. T. S. 1994, MNRAS, 268, 709
Brazier, K. T. S., et al. 1994, MNRAS, 268, 517
Buccheri, R., et al. 1978, Nature, 274, 572
———. 1983, A&A, 128, 2451
Buccheri, R., Özel, M. E., & Sacco, B. 1987, A&A, 175, 353
Chen, K., & Ruderman, M. 1993, ApJ, 402, 264
Cheng, K. S., Ho, C., & Ruderman, M. 1986, ApJ, 300, 500
Chiang, J., & Romani, R. W. 1992, ApJ, 400, 629
Daugherty, J. K., & Harding, A. K. 1982, ApJ, 252, 337
———. 1994, ApJ, 429, 325
De Jager, O. C., Swanepoel, J. W. H., & Raubenheimer, B. C. 1989, A&A, 221, 180
De Jager, O. C. 1994, ApJ, 436, 239
Dermer, C. D., & Sturner, S. J. 1994, ApJ, 420, L75
Fichtel, C. E., et al. 1994, ApJS, 94, 551
Fierro, J. M., et al. 1993, ApJ, 413, L27
———. 1994, ApJ, submitted
Frail, D. A., Kulkarni, S. R., & Vasisht, G. 1993, Nature, 365, 136
Halpern, J. P., & Holt, S. S. 1992, Nature, 357, 222
Halpern, J. P., & Ruderman, M. 1993, ApJ, 415, 286
Harding, A. K. 1981, ApJ, 245, 267
Harding, A. K., & Daugherty, J. K. 1993, in Isolated Pulsars, ed. K. A. Van Riper, R. Epstein, & C. Ho (Cambridge: Cambridge Univ. Press), 279
Helfand, D. J. 1994, MNRAS, 267, 490
Hermsen, W., et al. 1992, IAU Circ. 5541
Ho, C. 1993, in Isolated Pulsars, ed. K. A. Van Riper, R. Epstein, & C. Ho (Cambridge: Cambridge Univ. Press), 271
Hsu, J. J., & Arons, J. 1993, preprint
Hughes, E. B., et al. 1980, IEEE Trans. Nucl. Sci., NS-27, 364
Johnston, S., Manchester, R. N., Lyne, A. G., Kaspi, V. M., & D'Amico, N. 1994, MNRAS, submitted
Kanbach, G. 1989, in Gamma Ray Observatory Science Workshop Proc., ed. W. N. Johnson (NASA Goddard Space Flight Center), 2-1
Kanbach, G., et al. 1980, A&A, 90, 163
Kanbach, G., et al. 1988, Space Sci. Rev., 49, 69
———. 1994, A&A, in press
Kaspi, V. M. 1993, Ph.D. thesis, Princeton Univ.
Kaspi, V. M., Lyne, A. G., Manchester, R. N., Johnston, S., D'Amico, N., & Shemar, S. L. 1993, ApJ, 409, L57
Lyne, A. G., & Manchester, R. N. 1988, MNRAS, 234, 477
Mattox, J. R., et al. 1992, ApJ, 401, L23
———. 1994, ApJ, submitted
Matz, S., et al. 1994, ApJ, 434, 288
Mayer-Hasselwander, H. A., et al. 1994, ApJ, 421, 276
Middleditch, J., Deich, W., & Kulkarni, S. 1993, in Isolated Pulsars, ed. K. A. Van Riper, R. Epstein, & C. Ho (Cambridge: Cambridge Univ. Press), 372
Miller, M. C., & Hamilton, R. J. 1993, ApJ, 411, 298
Nel, H. I., & De Jager, O. C. 1994, in Proc. Second Compton Gamma Ray Observatory Symposium, ed. C. E. Fichtel, N. Gehrels, & J. P. Norris (AIP Conf. Proc), 91
Nolan, P. L., et al. 1993, ApJ, 409, 697
Oberlack, U., Diehl, R., Montmerle, T., Prantzos, N., & von Ballmoos, P. 1993, ApJS, 92, 433
Ögelman, H. B., et al. 1976, ApJ, 209, 584
Rankin, J. M. 1990, ApJ, 352, 247
Romani, R. W., & Yadigaroglu, I.-A. 1994, ApJ, submitted
Ruderman, M., & Cheng, K. S. 1988, ApJ, 335, 306
Smith, F. G. 1986, MNRAS, 219, 729
Sturner, S. J., & Dermer, C. D. 1994, ApJ, 420, L79
Taylor, J. H. 1989, in Gamma Ray Observatory Science Workshop, ed. W. N. Johnson (NASA Goddard Space Flight Center), 4-143
Taylor, J. H., & Cordes, J. M. 1993, ApJ, 411, 674
Taylor, J. H., Manchester, R. N., & Lyne, A. G. 1993, ApJS, 88, 529
Thompson, D. J. 1993, in Isolated Pulsars, ed. K. A. Van Riper, R. Epstein, & C. Ho (Cambridge: Cambridge Univ. Press), 385
Thompson, D. J., et al. 1977, ApJ, 213, 252
———. 1983, A&A, 127, 220
———. 1992, Nature, 359, 615
———. 1993, ApJS, 86, 629
Ulmer, M. P. 1994, ApJS, 90, 789
Ulmer, M. P., et al. 1993, ApJ, 417, 738
Ulmer, M. P., & Schroeder, P. C. 1994, in Proc. Conf. Lives of Neutron Stars, Kemer, Turkey, in press
Wilson, R. B., et al. 1993, in Isolated Pulsars, ed. K. A. Van Riper, R. Epstein, & C. Ho (Cambridge: Cambridge Univ. Press), 257